

## FORMULATION AND EVALUATION OF EPIGALLOCATECHIN GALLATE AND BERBERINE-LOADED CHITOSAN NANOPARTICLES

GOPU VIJAYA SINDHURI<sup>1</sup>, GURUSAMY MARIAPPAN<sup>2</sup>, SELVAMUTHUKUMAR SUBRAMANIAN<sup>1\*</sup>

<sup>1</sup>Department of Pharmacy, Annamalai University, Annamalai Nagar 608002, Tamil Nadu, India. <sup>2</sup>Department of Pharm Chemistry, St Mary's College of Pharmacy, Secunderabad 50002, Telangana, India  
\*Email: smk1976@gmail.com

Received: 23 Dec 2022, Revised and Accepted: 14 Mar 2023

### ABSTRACT

**Objective:** The current work aimed to prepare and characterize epigallocatechin gallate (EGCG)+berberine-loaded chitosan nanoparticle (EBNP).

**Methods:** The ionic gelation method was adopted. A batch of 17 nanoformulations was prepared by using chitosan as a natural biodegradable polymer and EGCG+berberine as active drug content and characterized.

**Results:** The SEM data proved that the chitosan-based nanoparticles were formed successfully with a spherical shape at 272 nm along with PDI 0.346. The FT-IR spectra confirmed that no drug-polymer interaction was observed. The DSC data proved that the formation of nanoparticles due to the presence of endothermic sharp melting points at 246 °C and 332 °C for EGCG and berberine in the pure form of the drug, whereas the same is absent in nanoformulation. The optimized formulation showed a percentage entrapment efficiency (% EE) for EGCG is 83.91 % and berberine at 90.62%, ZP of the nanoparticle is 11 mV.

**Conclusion:** This study demonstrated that box-behnken designs can optimize the formulation and the process variables to achieve favorable responses. Hence, it can be concluded that the best-optimized nanoparticle formation was confirmed and characterized.

**Keywords:** Epigallocatechin gallate, Berberine, Nanoparticle and chitosan

© 2023 The Authors. Published by Innovare Academic Sciences Pvt Ltd. This is an open access article under the CC BY license (<https://creativecommons.org/licenses/by/4.0/>)  
DOI: <https://dx.doi.org/10.22159/ijap.2023v15i3.47410>. Journal homepage: <https://innovareacademics.in/journals/index.php/ijap>

### INTRODUCTION

Nanotechnology plays a key function to convert large structures into nanostructures [0.1-100 nm]. Due to its improved bioavailability, nanotechnology is being successfully used to deliver medications to their intended sites [1, 2]. Polymeric NPs, ceramic NPs, and metallic NPs are a few forms of NPs obtained from polymers such as alginate, xanthan gum, chitosan, PVA, PLGA, and PEG have been employed [3, 4]. The NPs controlled drug distribution benefits them, improving stability and minimizing negative effects [5]. Chitosan is a natural polymer for nanotechnology research because of its biocompatibility, bio-reducibility, and low toxicity [6-9]. Drugs with pre-systemic effects can be delivered mucosally, which has certain particular advantages over oral administration. Several techniques, including emulsion droplet coalescence, reverse micelle synthesis, polyelectrolyte complexation, emulsion solvent diffusion, ionic gelation, and desolvation, have been reported for the generation of

NPs [10, 11]. The mean particle size, zeta potential, PDI, and entrapment efficiency are characterized to confirm the formulation. Biodegradable hydrophilic polymers like chitosan, gelatin, and sodium alginate are generally employed to create NPs utilizing the ionic chelation process with cross-linking chemicals like sodium tripolyphosphate or glutaraldehyde [12]. Keeping this view in mind, in this present study epigallocatechin gallate and berberine were used to prepare nanoformulation. Berberine is an alkaloidal substance that is commonly used to treat cancer, inflammation, diabetes, viral infections, and bacterial infections [13-16]. Epigallocatechin gallate (EGCG) is a polyphenolic substance can be found in both green and black tea. It is currently being researched as a neuroprotective and anticancer Hsp90 inhibitor [17-20]. The chemical structure of both EGCG+Berberine is given in fig. 1. Based on the above facts, the present study was designed to prepare chitosan-based nanoformulation and its characterization by DSC, SEM, and FT-IR etc.

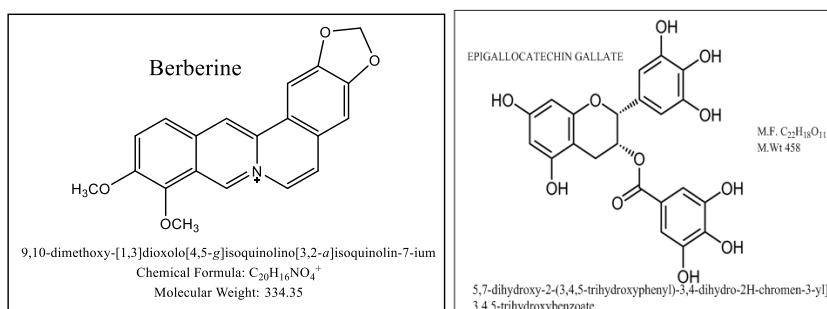


Fig. 1: Structure of berberine and epigallocatechin gallate

### MATERIALS AND METHODS

The EGCG and berberine were purchased from Sigma Aldrich. All other solvents and chemicals used were of analytical grade. Scanning electron microscopy (SEM; JEOL JMS-6390 apparatus) at 25±2 °C

was used for recording the image of the nanoparticle. A Differential Scanning Calorimeter (DSC 6000-PerkinElmer) was used for DSC analysis. The IR spectra were recorded by IR spectrometer (Shimadzu Corporation, Kyoto, Japan). All the HPLC analysis was carried out by HPLC (Shimadzu LC-2030C prominence-I (Japan).

## Preparation of chitosan nanoparticles

### Preparation of chitosan solution

Chitosan solution was prepared by dispersing 100 mg of chitosan in 100 ml of glacial acetic acid solution (1%) while stirring continuously for three hours. The mixture was then filtered through a PVDF syringe filter with a 0.22 µm pore size. In addition, the produced solution was left overnight to create a clear solution.

### Ionic gelation method

The chitosan-based nanoparticles were prepared based on the ionic gelation of chitosan with sodium tripolyphosphate (TPP) anions. EGCG and Berberine with constant concentration (50 mg each) were added to different concentrations of the polymer prepared from the above chitosan solution. The cross-linking of chitosan with TPP at equal volume was performed drop by drop under a magnetic stirrer at 1000 rpm. The resulting formulation was centrifuged for 10 min at 10,000 rpm, and the pellet was suspended in sterile distilled water followed by ultra-sonication for 100 seconds at 4 °C for further analysis [21, 22].

### Experimental design

Most formulation experiments vary one element (or variable) at a time while maintaining the status quo for other factors. When all elements are changed at once, as is possible with a factorial design, the effects of independent variables and their interactions may be quantified. By selecting the chitosan concentration (C), TPP concentration (TP), drug concentration (D), stirring speed (SS), and stirring time (ST) as independent variables, the experimental design was used in this study to optimize the formulation of nanoparticles. The studies were carried out with three levels of three variables [23]. The analysis of variance (ANOVA) approach was used to statistically evaluate the data, and the findings were presented as mean, standard deviation.  $P < 0.05$  was used as the threshold for significance.

### Optimization of nanoparticles by scanning electron microscope (SEM)

The particle shape and surface characteristics of the freshly prepared nanoparticle formulations were investigated by scanning electron microscope (SEM) Scanning electron microscopy (SEM; JEOL JMS-6390 apparatus) at  $25 \pm 2$  °C.

### Differential scanning calorimetry (DSC)

The structural and crystallinity changes in EGCG+berberine and the polymer due to the thermal impacts during the formulation steps were evaluated using differential scanning calorimetry (Perkin Elmer Differential Scanning Calorimeter (DSC 6000-PerkinElmer)). Ten milligrams of the samples were accurately weighed in aluminum pans and heated from 25 to 500 °C at a heating rate of 20 °C  $\text{min}^{-1}$  under a continuous nitrogen flow.

### FT-IR analysis

Fourier Transform Infrared (FT-IR) analysis spectra were recorded using a Shimadzu IR (Shimadzu Corporation, Kyoto, Japan) at the wavelength range of 4000-500  $\text{cm}^{-1}$ .

### Particle size, polydispersity index and zeta potential analysis

Particle size, PDI, zeta potential of the prepared nanoparticles were analyzed by Dynamic light scattering technique using Malvern zeta size Nano ZS 90 (Malvern instrument UK). The Nano formulation was dissolved with distilled water (1:10). 1 ml of the dil. the sample was analyzed by using Zeta sizer at 25 °C. Each sample was analyzed in triplicate as  $\text{mean} \pm \text{SD}$ .

### Entrapment efficacy (% EE)

The entrapment efficacy of nanoformulation was determined by measuring the untrapped drug by using the centrifugation method. The nanoparticle samples were centrifuged at 1000rpm at 4 °C for 15 min. The amount of EGCG+Berberine was collected diluted with methanol and analyzed by HPLC and 205 and 230 nm. The % EE was expressed as follows.

$$\% \text{ EE} = \frac{\text{Total concentration of drug} - \text{Free conc of drug}}{\text{total conc of drug}}$$

The analysis was done in triplicate; the results were expressed as  $\text{mean} \pm \text{SD}$

### Drug release studies by HPLC

The release behavior of nanoparticles was studied using a dialysis membrane technique. The 10 h duration, the *in vitro* release profiles of EBNP in freshly made simulated intestinal fluid (SIF, pH 6.8) were examined. In a nutshell, dialysis bags (with a molecular cut-off of 12-14 kD, Sigma) were filled with drug-loaded nanoparticles and sealed with closures. In a water bath at 37 °C, the bags were submerged in a dissolving media containing 80 ml of SIF while being continuously magnetically stirred at a rate of 100 rpm. The Concentration of EGCG+berberine in the receptor chamber was then evaluated by HPLC (Shimadzu LC-2030C prominence-I (Japan)). Subsequent 1-ml samples were taken at predefined time intervals. The receptor compartment was kept in sink conditions throughout the *in vitro* release experiments. Three times each experiment was carried out.

### Stability studies

The generated EBNPs formulations were tested for three months of stability, and samples were kept at 4 °C in sealed amber-colored glass vials. The samples were evaluated for particle size, ZP, EE, and drug loading after three months.

## RESULTS AND DISCUSSION

### Statistical analysis of formulations

The results obtained from all 17 formulations were analyzed by using design-expert version 11.0 software. programme was used to construct appropriate research designs and response surface plots, and a numerical optimization technique was used to produce new formulations with desirable responses. The elicited responses were put to use to research the impact of independent variables. For particle size, ZP, and % entrapment efficiency, a quadratic model was proposed. The software generated a list of solutions, and those that met the necessary criteria were reported and ordered in descending order of desirability. Using analysis of variance, the factors that had a significant impact on the responses were found (ANOVA). The optimum formulation was created by following the solutions found and evaluated using the predetermined criteria. The experimental values that were obtained were compared to the predicted values. Based on the report from design expert software, the formula for the best formulation i.e. F18 was predicted and prepared for further studies [Table 1 and 1.1and 1.1a].

### Optimization and validation

To find out the optimal formulation, Design-expert software was used to analyze the desirability function. The smallest size of solid lipid nanoparticles include ZP, the ideal poly dispersibility index, and the highest drug entrapment efficiency were the requirements for the optimization. The software's answers were saved in descending order of desirability, and the formulation with the highest factor of desirability was chosen. Predicted values and actual values were compared using the formulation, and the relative error was calculated. The batch's minimal relative error was determined to be less than 5%.

### Differential scanning calorimetry

It is a very important analytical tool to investigate the melting and recrystallization behavior of solid nanoparticles. It revealed the thermogram of pure EGCG, berberine, a combination of both and a chitosan-based nanoparticle of EGCG+berberine (EBNP). Fig. 2 shows the DSC thermogram of EGCG that describes the sharp endothermic peak of EGCG is 246 °C. Fig. 2.1 shows the peak at 332 °C, which corresponds to the crystalline nature of berberine. These sharp endothermic melting points indicated that both EGCG and berberine are crystalline in nature. Fig. 2.2 did not show any peak in the endothermic region that confirms the amorphous state of both drugs. From this observation, it can be concluded that both drugs are uniformly dispersed, which is a unique characteristic feature of the formation of the nanoparticle [24].

Table 1: 3D factorial design with values of an independent variable and possible nanoformulations

Std	Run	Factor 1 X1	Factor 2 X2	Factor 3 X3	Response 1	Response 2	Response 3	Response 3
		A: Chitosan	B: TPP	C: Stirring speed	PS Y1	ZP Y2	EE (EGCG) Y3	EE (berberine) Y3
		%	%	RPM	nm	mV	%	%
7	1	1	1	1000	350	5	53	76
1	2	1	0.5	750	150	10	58	62
17	3	1.5	1	750	270	12	86	91
11	4	1.5	0.5	1000	190	10	41	80
14	5	1.5	1	750	270	12	86	91
10	6	1.5	1.5	500	120	5	72	42
8	7	2	1	1000	240	4	81	50
2	8	2	0.5	750	350	18	90	69
9	9	1.5	0.5	500	80	19	32	75
12	10	1.5	1.5	1000	240	21	64	79
4	11	2	1.5	750	450	2	84	71
13	12	1.5	1	750	270	12	86	91
5	13	1	1	500	220	6	43	61
6	14	2	1	500	510	9	70	49
3	15	1	1.5	750	330	5	59	67
16	16	1.5	1	750	270	12	86	91
15	17	1.5	1	750	270	12	86	91

Table 1.1: Variable selection and their usage in 3<sup>3</sup> factorial design

Name	Unit	Type	Lower level (-1)	Higher level (+1)
chitosan (X1)	%	Factor	1	2
TPP (X2)	%	Factor	0.5	1.5
RPM (X3)	-	Factor	500	1000
Particle size (Y1)	nm	Response		
Zeta potential (Y2)	mV	Response		
% EE (Y3)	%	Response		

Table 1.1a: The predicted best nanoformulation and the effects of variable factors on response

Factor 1	Factor 2	Factor 3	Response 1	Response 2	Response 3	Response 3
A: Chitosan	B: TPP	C: Stirring speed	PS Y1	ZP Y2	EE (EGCG) Y3	EE (berberine) Y3
%	%	RPM	nm	mV	%	%
1.41	1.11	733	270	11	83.91	90.62

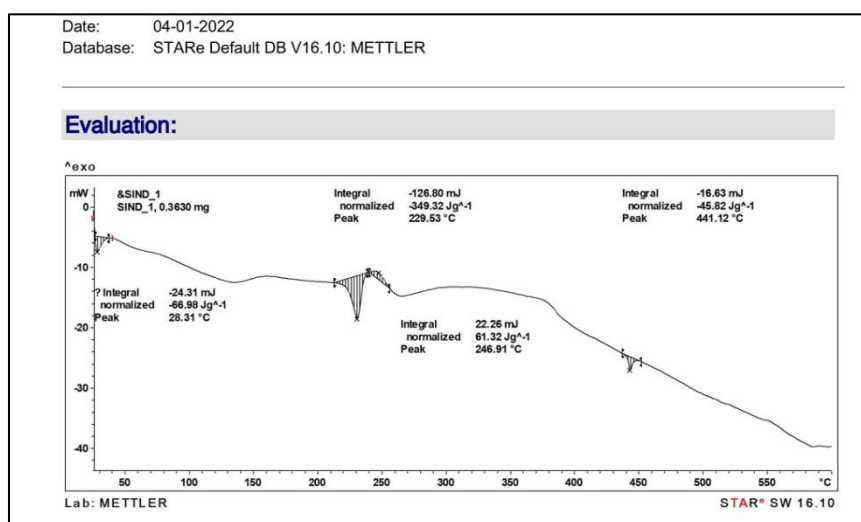


Fig. 2: DSC Thermogram of EGCG

### IR analysis

FT-IR Analysis was done to ascertain the interaction of EGCG+berberine combination with chitosan polymer. The IR Spectra recorded for EGCG had shown the characteristic peaks at 3414 cm<sup>-1</sup> for the OH group 1599 cm<sup>-1</sup> for the C=O group, 1207 cm<sup>-1</sup> for CH<sub>2</sub>- for 1388

and 1508, 1331, 1105, 712 cm<sup>-1</sup> for Ar ring vibrations. Similarly berberine had shown the peaks at 2922 cm<sup>-1</sup> (OMe), 1506(C=N)-O-C-O-(1105 cm<sup>-1</sup>) along with Aromatic ring vibrations at 1599 cm<sup>-1</sup>, 1388 cm<sup>-1</sup>, 1362 cm<sup>-1</sup>, 1036, 712 cm<sup>-1</sup>. The chitosan polymer had shown peaks at NH<sub>2</sub>-3432 OH-3432, C-O-C-1153, and CH<sub>2</sub>-2921 cm<sup>-1</sup>. The peak at 3432 resulted due to the OH group, which overlapped with the

NH<sub>2</sub> group of chitosan. The appearance of peaks at 3355, 3402, 2945, 1601, and 1506 cm<sup>-1</sup> confirmed that both drugs berberine and EGCG did not have any chemical interactions with respect to their functional groups. This was confirmed by the appearance of sharp peaks at respective wave numbers for respective functional groups such as OH, NH<sub>2</sub>, C=N, C=O, C-O-C and aromatic ring vibrations in the IR spectrum

of both compounds. The presence of peaks at 3431, 2922, 1631, and 1026 confirmed that no drug-polymer interaction was observed. Finally, the IR spectrum of both drug+polymer was recorded. The appearances of characteristic peaks present in both compounds were also present with a slight shift in wave number. This confirmed that no drug-polymer interaction observed [fig. 3, 3.1, 3.2, 3.3].

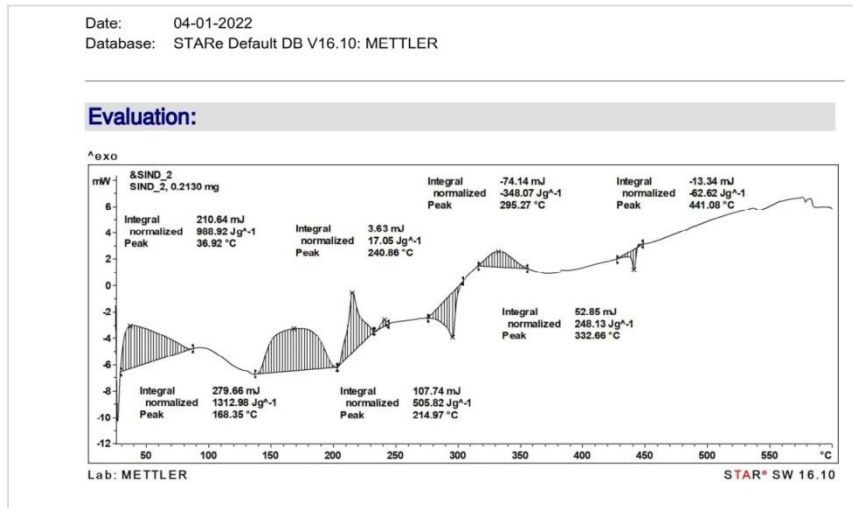


**Fig. 2.1: DSC thermogram of berberine**

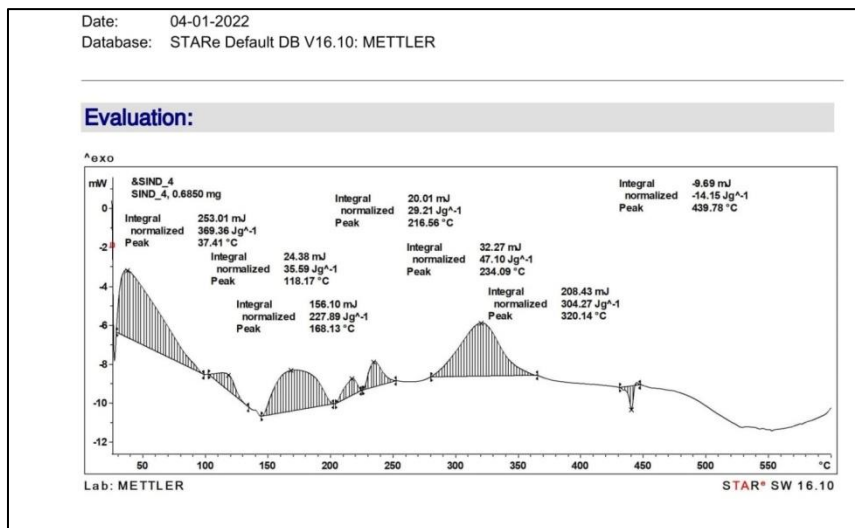


**Fig. 2.2: DSC thermogram of nanoparticle**

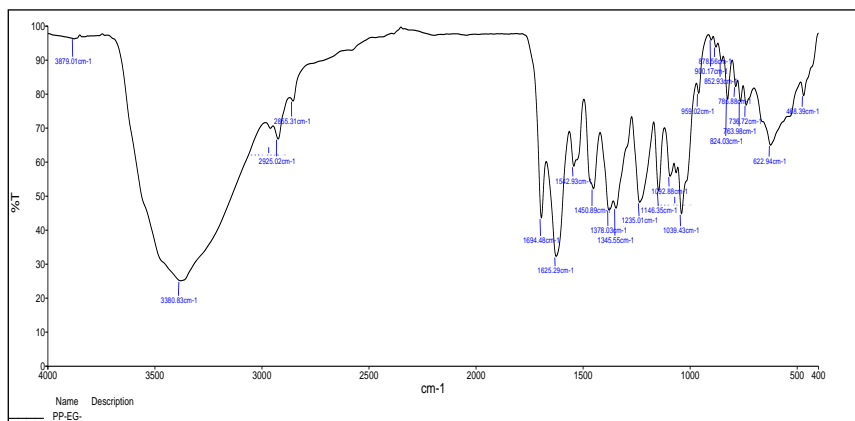


**Fig. 3: FT IR spectrum of EGCG**

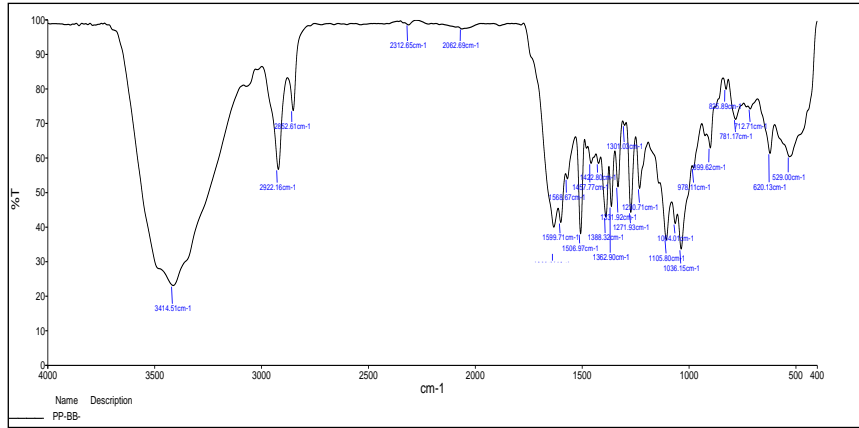


Fig. 3.1: FT IR spectrum of berberine

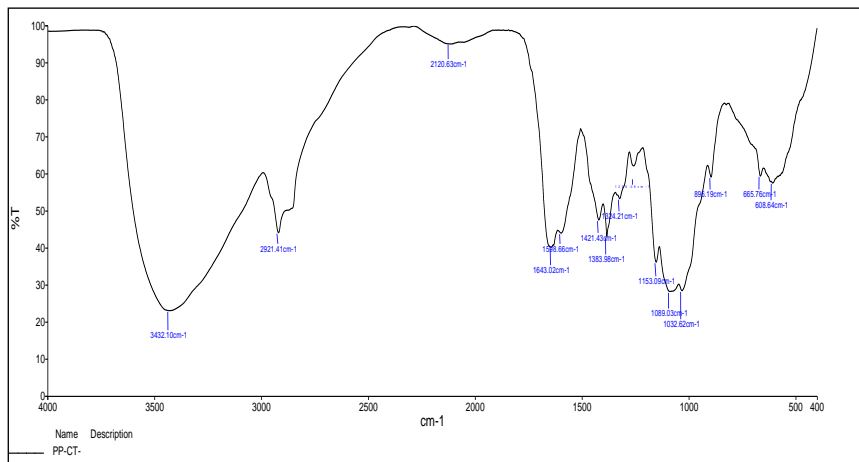


Fig. 3.2: FT IR spectrum of chitosan

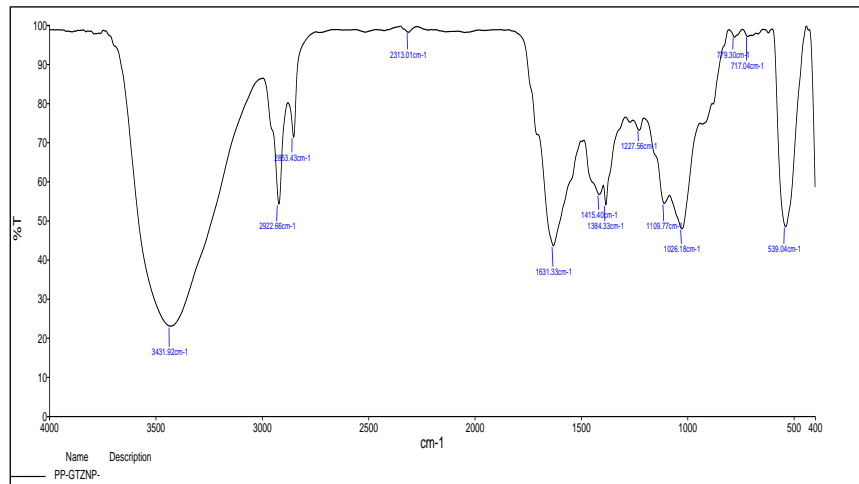


Fig. 3.3: FT IR spectrum of EGCG+berberine+chitosan polymer combination

**Effect on particle size (PS)**

The particle size varied from 80 nm to 510 nm (formulation 1-17) for various factor-level combinations. The effects of polymer concentration, TPP concentration, and stirring speed as independent factors (variables) impacting particle size were investigated. The suggested quadratic model with an F-value of 5.36 implies that the model was significant. The model P value was <0.01, indicating that the model terms are significant. P values for the polymer-to-drug

ratio was 0.0002; polymer concentration was <0.0001. The result indicated that there was no significant difference in particle size with the change in homogenization time. The regression coefficient value  $R^2$  was 0.9461, adjusted  $R^2$  was 0.7105 and predicted  $R^2$  was 0.8652 indicating minimum variations in the experimental model.

A ratio greater than 4 is desirable, and this model can be used to navigate the design space. The polynomial equation in terms of coded factors is given below.

$$PS = +270 + 62.50 A + 46.25 B + 11.25 C - 20 AB - 100 AC + 2.50 BC + 111.25 A^2 - 61.25 B^2 - 51.25 C^2$$

A= chitosan polymer, B= TPP, C=stirring speed

The individual factor A had a positive effect on particle size shown by the positive coefficient estimate value. From the equation, it can be understood that the particle size has a linear relationship with the

concentration of polymer, the concentration of TPP, and stirring speed. Since the coefficient of A and B are showing positive value, the particle size increased with the ratio of polymer to the drug, whereas TPP Concentration showed a positive effect and homogenization time showed a negative effect. The effect of polymer: drug ratio, homogenization time, and polymer concentration on the particle size were presented in the form of response surface plots [fig. 5].

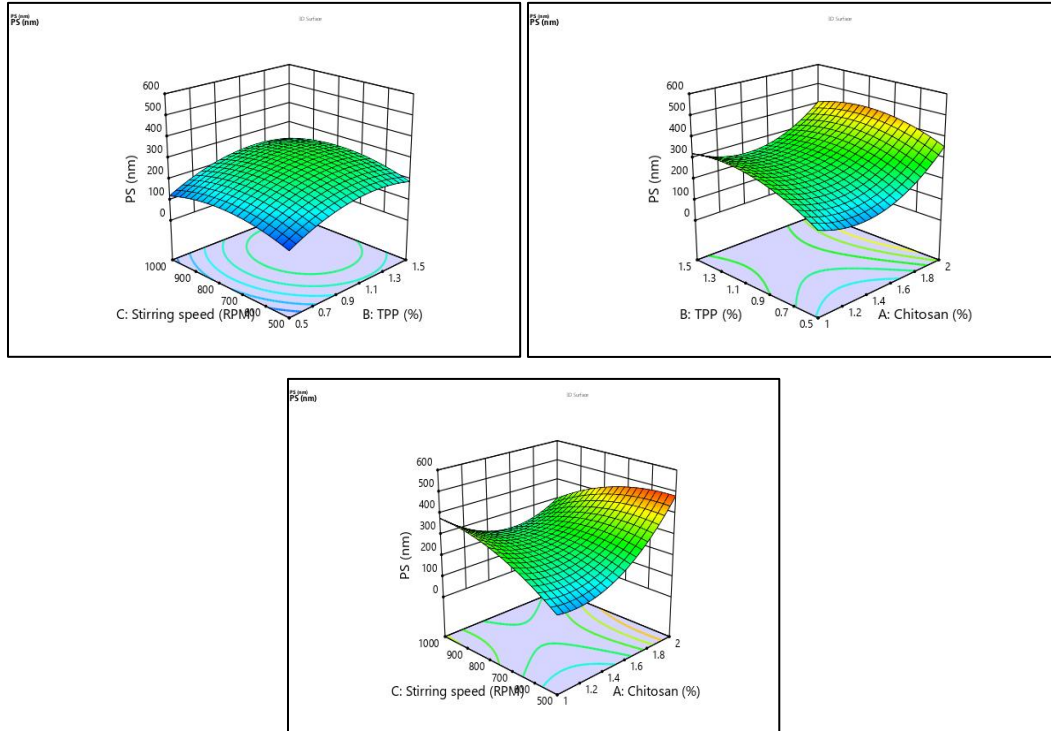


**Fig. 5: 3D surface plot for the effect of independent variable on particle size**

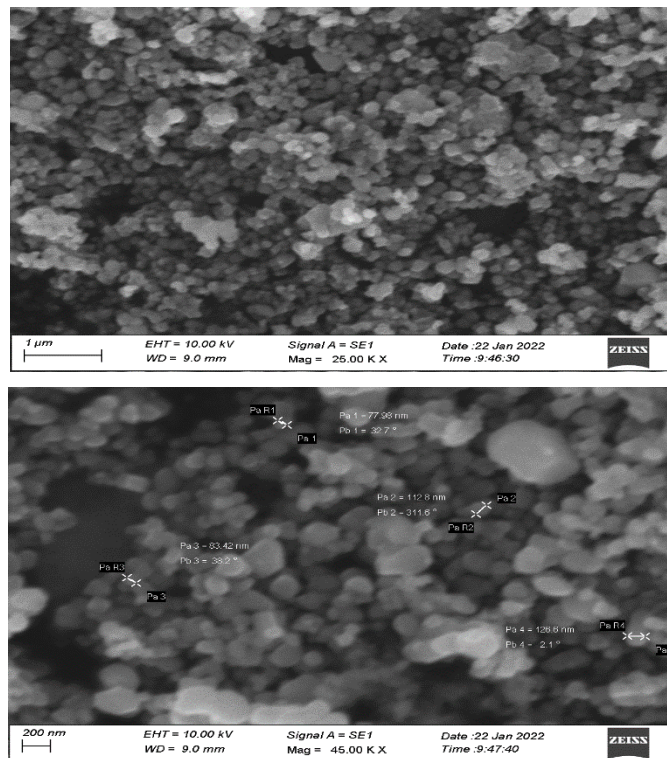


**Fig. 4: SEM image of nanoparticle of EGCG+berberine at 1 μm and 200 nm**

The size and shape of the nanoparticle were evaluated by SEM. [fig. 4] The SEM image of the nanoparticles was confirmed by the oval and spherical shape with narrow size distribution. Fig. 4.1 showed the SEM image of the nanoparticle. Moreover, the particles are not in the aggregated state. The observed diameter of the nanoparticles is

in agreement with the data from the Malvern particle size analyzer. From the particle size analysis and intensity distribution, the polydispersity index from the nanoformulation was found to be 0.346 with a diameter 272 nm. The PDI value 0.346 implied that the sample is mono dispersed in nanoformulation.

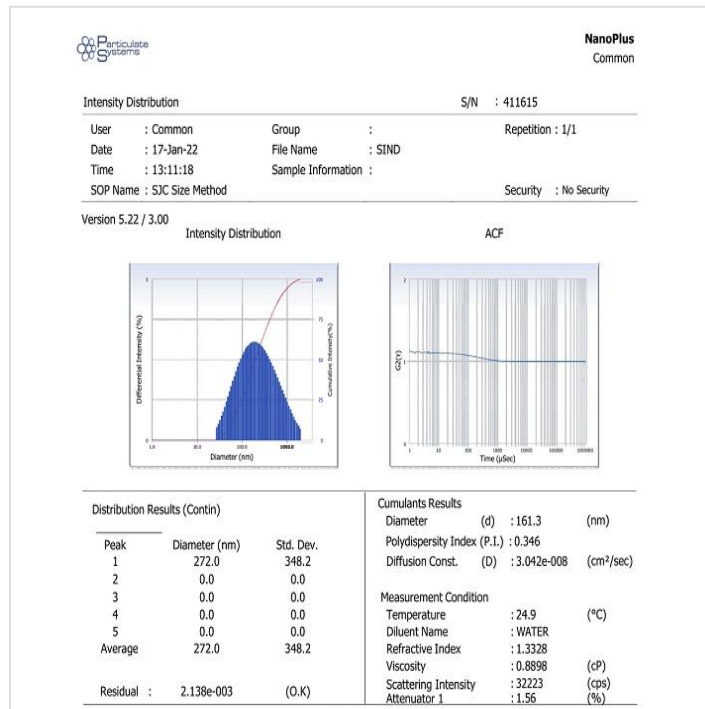


**Fig. 4.1: Particle size analysis data of nanoformulation**

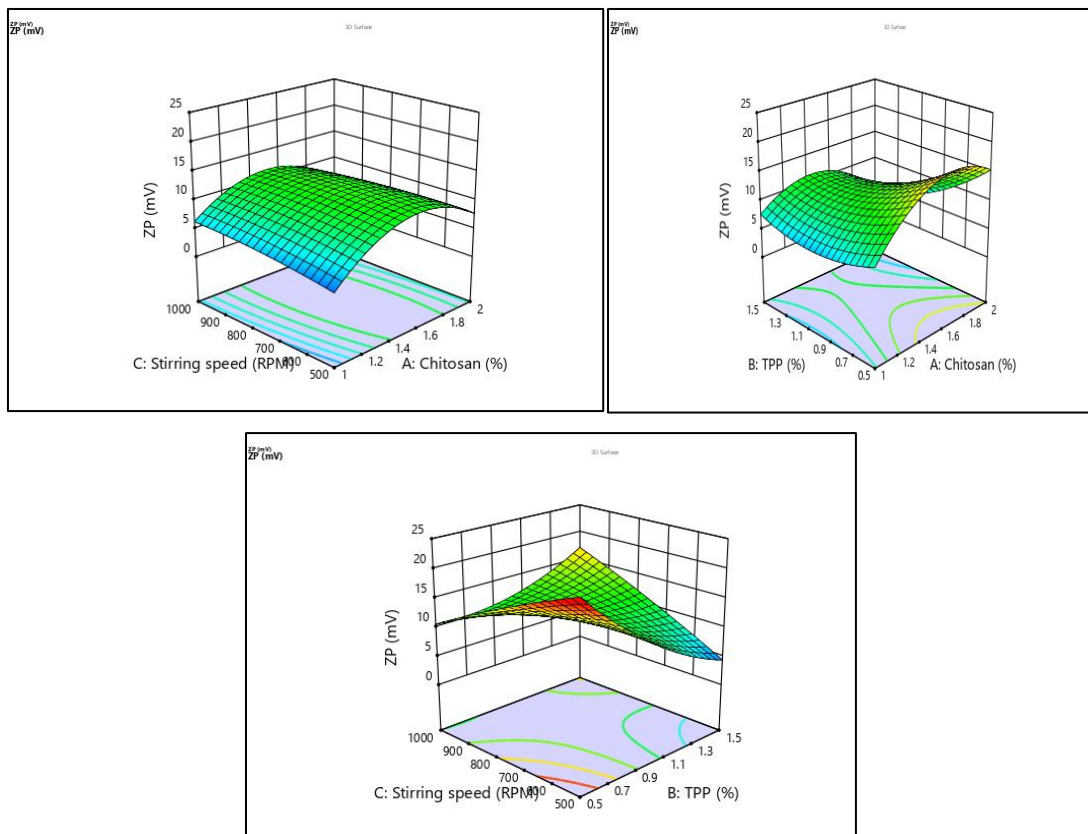


**Fig. 5.1: 3D surface plot for the effect of an independent variable on zeta potential**

### Effect on zeta potential

The zeta potential for EBNP is an important parameter, as it shows the stability of the formulation. The positive zeta potential of all formulations showed the stability of the NPs. The zeta potential of the 17 formulations ranged from 2 to 21 mV. Based on the  $r^2$  value (0.6993), the quadratic model was fitted with the following regression equation: [fig. 5.1].

$$ZP = +12 + 0.8750 A - 3 B + 0.1250 C - 2.75 AB - 1 AC + 6.25 BC - 5.50 A^2 + 2.25 B^2 - 0.5000 C^2$$

From the quadratic model, it has been found that the zeta potential for the nanoformulation was 11mV. A high positive zeta potential is required for effective cell contact and to encourage intracellular transport of the nanoparticulate chitosan system [25]. Zeta potential testing is a crucial metric for assessing the stability of the formulation for nanoparticles. Large absolute zeta potential values indicate drug-loaded nanoparticles with high electric surface charges, which might provide strong repulsive forces between the particles to avoid aggregation [26].

### Effect on % EE

The suggested quadratic model for EGCG with an F-value of 6.45 implied that the model was significant. The model-free P value was <0.05, indicating that the model terms are significant. P values for, polymer to drug ratio was 0.004, polymer concentration was 0.0067, and that for homogenization time was <0.0001. The results indicated that there was no significant difference in % EE with the change in homogenization time. The regression coefficient value  $R^2$  was 0.9504, adjusted  $R^2$  was 0.9420, and predicted  $R^2$  was 0.7971

indicating minimum variations in the experimental model and this model can be used to navigate the design space. The polynomial equation in terms of coded factor is given below. (fig. 5.2 and 5.3). Similarly, the study was done for berberine; the quadratic model with F value for berberine is 4.59 confirmed the model is significant with a P value of 0.00285. The P value for chitosan was 0.004, TPP 0.03 stirring speed was 0.06.

$$EE(EGCG) = +86 + 14A + 7.25B + 2.75C - 1.75AB + 0.2500 AC - 4.25 BC - 1.87A^2 - 11.37B^2 - 22.38 C^2$$

$$EE(\text{berberine}) = +91 - 3.38A - 3.37B + 7.25C - 0.7500AB - 3.50AC + 8.00BC - 16.88A^2 - 6.88B^2 - 15.12C^2$$

The entrapment efficiency of berberine can be increased by decreasing the polymer concentrations and concentration of TPP since it shows the negative coefficient in the above equation. A= chitosan polymer, B= TPP, C=stirring speed

All three factors were significant in the entrapment of EGCG+berberine in chitosan NPs. The highest positive coefficient with berberine indicated that as the drug concentration increases, entrapment also increases. Smaller particles possess a large surface and more drugs were entrapped into the particles than in chitosan nanoparticles, which showed entrapment efficiencies of 83.91% for EGCG and 90.62 % for berberine. The equation in terms of coded factors can be used to make predictions about the response to given levels of each factor. By default, the high levels of the factors are coded as +1 and the low levels are coded as -1. The coded equation is useful for identifying the relative impact of the factors by comparing the factor coefficients.

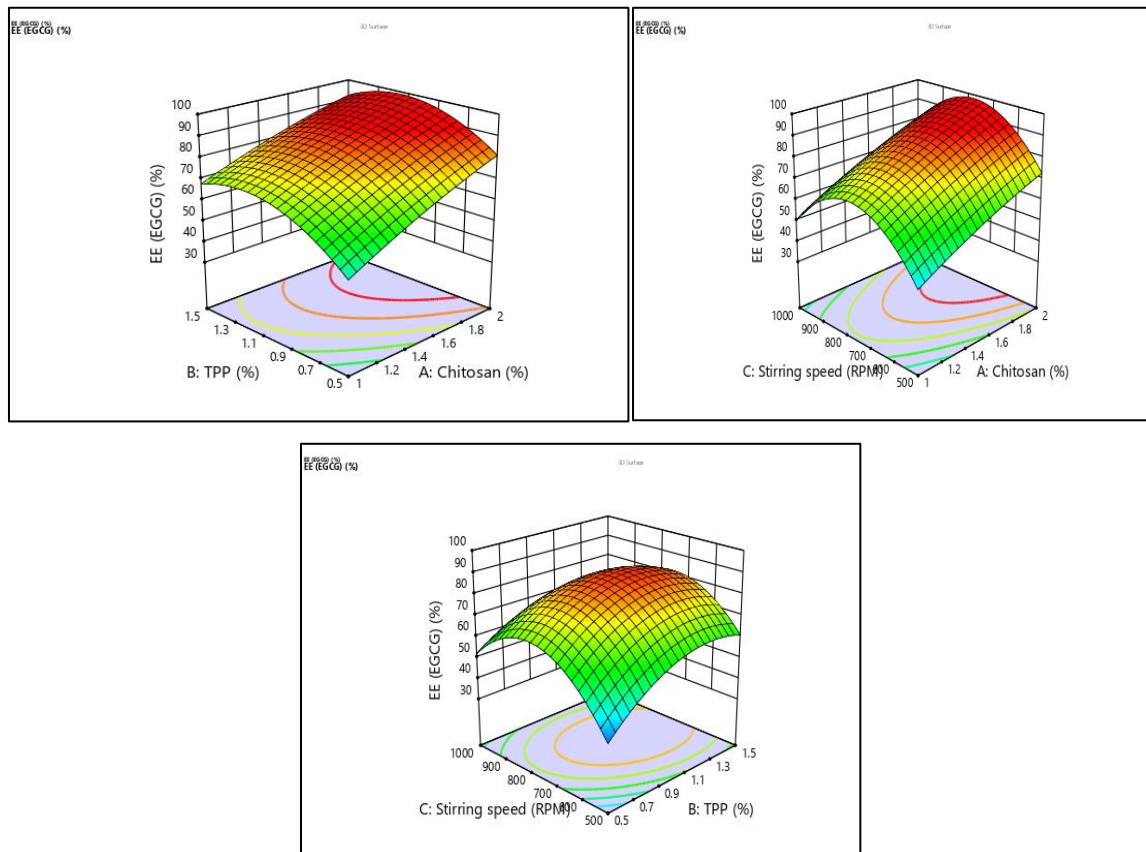


Fig. 5.2: 3D surface plot for the effect of an independent variable on entrapment efficiency (EGCG)

### Desirability

Desirability is an objective function that ranges from zero outside of the limits to one at the goal. The numerical optimization finds a point that maximizes the desirability function.

A desirability of 1.00 means the goals were easy to reach and better results [27]. Based on the results from the 3D graph, the desirability function is 0.836 which ascertained that all the functions used in this study are within the permissible limit [fig. 5.4].

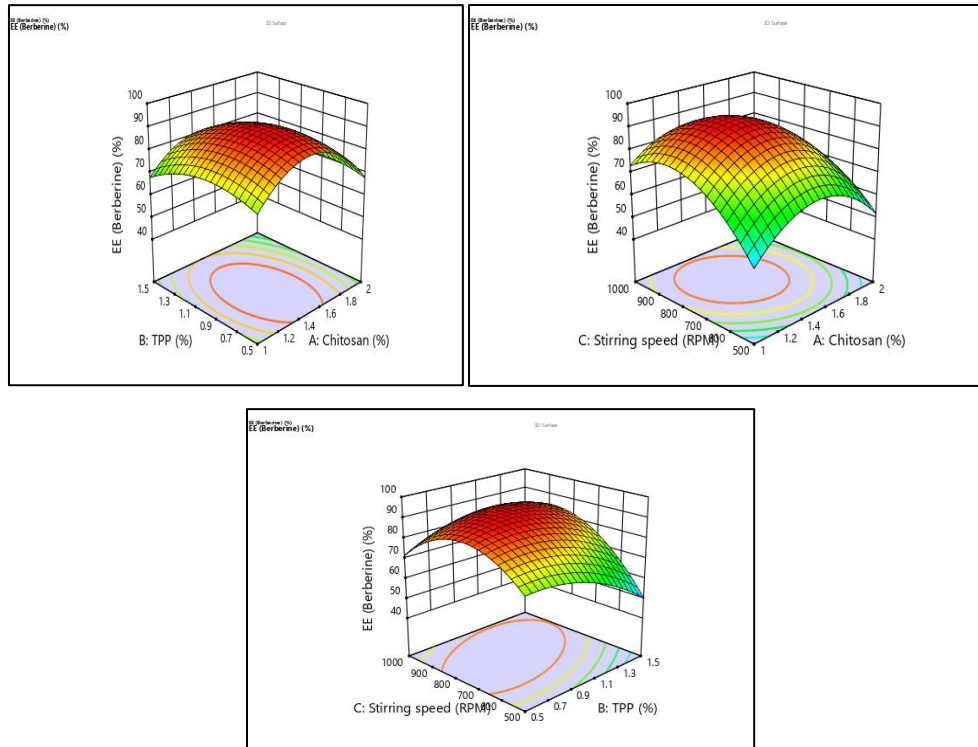


Fig. 5.3: 3D surface plot for the effect of independent variable on entrapment efficiency (berberine)

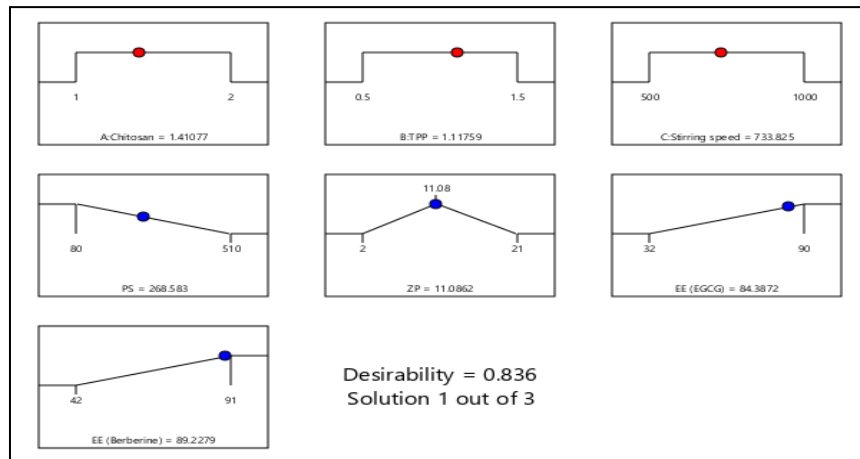


Fig. 5.4: Desirability plot

**Drug release studies**

The *in vitro* drug release studies of EGCG were carried out from the 300µg-1500µg/ml concentration range. The graph was plotted against concentration vs area. The R<sup>2</sup> value 0.9972 proved that the graph obeyed the linearity (fig. 6, 6.1, 6.2, 6.3). The concentration of the drug release profile was studied within the particular time frame. The HPLC results demonstrated that the drug (EGCG) is released gradually to time for example: at 1 h. 14.02%; 2 hr. 24.68% and so on [table 2, 2.1, 2.2]. Similarly, study was performed to assess the release profile of berberine and showed that the graph obeyed linearity with an R<sup>2</sup> value 0.9776. Interestingly the drug also released in linearly with respect to time i.e. 1h 16.25%, 2h 23.87%, and 10hr. 95.23%. The report from HPLC demonstrated that both the drugs EGCG and berberine loaded in chitosan, nanoparticles expressed uniform release profile and were also present within the acceptable range [Table 3, 3.1, 3.2]. There are several methods by which drugs are released from nanoparticles, including surface

erosion, disintegration, diffusion, and desorption [28]. Chitosan nanoparticles with EBNP loaded revealed an initial release of 16.25% and 14.02, respectively, which might be explained by berberine and EGCG adsorbed to the surface. 95.23% and 94.08% of both drugs were released over 10 h. The swelling feature of the polymer causes an enhanced release in aqueous solutions with respect to time.

Table 2: Std calibration graph conc vs area

Con (mcg/ml)	Area
300	4025467
600	8133815
900	12168541
1200	17632396
1500	21776294

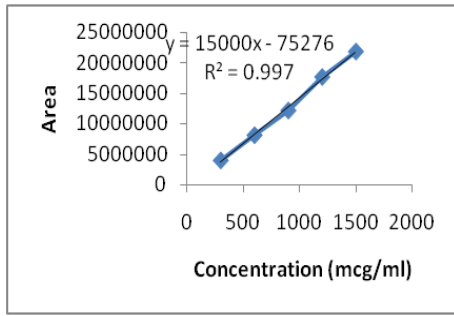


Fig. 6: Std calibration graph by HPLC

Table 2.1: *In vitro* release profile of EGCG

Time (h)	% Drug release
0	0
1	14.02±0.10
2	24.68±0.21
3	40.15±0.16
4	53.62±0.23
6	73.41±0.36
8	86.89±0.41
10	94.08±0.11

Data are expressed mean±SD (n=3)

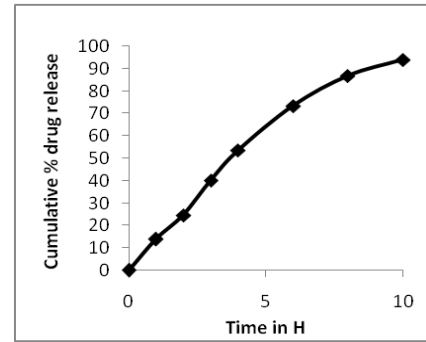


Fig. 6.1: Diffusion study profile

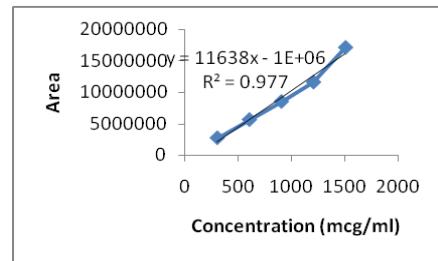


Fig. 6.2: Std calibration graph by HPLC

Table 2.2: *In vitro* release profile of EGCG

Time (H)	Sample area	Conc (mcg/ml)	Conc (mg)	Con inc 900 ml	release	% Release
0	0	0	0	0	0	0
1	116833.333	7.788888889	0.007789	7.01	0.1402	14.02
2	205666.667	13.711111111	0.013711	12.34	0.2468	24.68
3	334583.333	22.305555556	0.022306	20.075	0.4015	40.15
4	446833.333	29.788888889	0.029789	26.81	0.5362	53.62
6	611750	40.783333333	0.040783	36.705	0.7341	73.41
8	724083.333	48.272222222	0.048272	43.445	0.8689	86.89
10	784000	52.266666667	0.052267	47.04	0.9408	94.08

Table 3: Std calibration graph conc vs area

Con (mcg/ml)	Area
300	2704141
600	5613377
900	8512825
1200	11619900
1500	17158030

Table 3.1: *In vitro* release profile of berberine

Time (h)	% Drug release
0	0
1	16.25±0.22
2	23.87±0.19
3	34.64±0.30
4	50.98±0.17
6	71.23±0.33
8	83.42±0.17
10	95.23±0.28

**Stability study**

The stability studies were carried out to assess the stability and integrity of chitosan-loaded NPs. The EBNP-loaded NPs showed minor changes in % content and release profile from 30, 60 and 90 d at 4 °C. The stability study results showed that the % drug content for EGCG was 96.04%, 95.26% and 94.05% after 30 d, 60

d, and 90 d, respectively. Similarly, for % drug release is 94.08%, 93.87%, and 93.14%. A similar kind of results was observed for berberine i.e. % drug release is 95.23%, 94.98%, and 93.71% at 30, 60, 90 d intervals, respectively. The data showed that there was a slight reduction in % drug content and percentage release. The difference in percentage drug content and release in both drugs was±1% only. The changes were insignificant, which indicated good physical stability of the NPs during their storage at 4 °C for three months [Table 4 and 5].

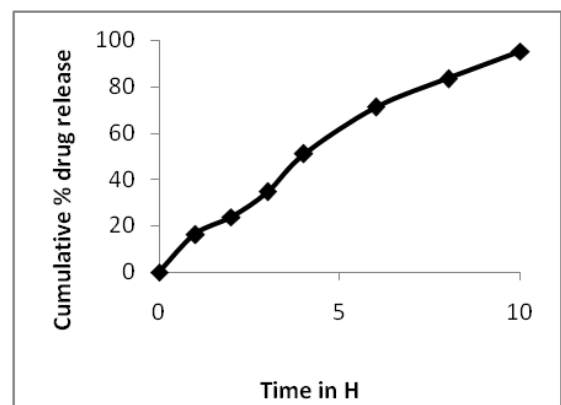


Fig. 6.3: Diffusion study profile of berberine data are expressed mean±SD (n=3)

Table 3.2: *In vitro* release profile of berberine

Time (H)	Abs	Conc (mcg/ml)	Conc (mg)	Concin 900 ml	Release	% release
0	0	0	0	0	0	0
1	105065.3	9.027778	0.009028	8.125	0.1625	16.25
2	154332.8	13.26111	0.013261	11.935	0.2387	23.87
3	223966.8	19.24444	0.019244	17.32	0.3464	34.64
4	329614	28.32222	0.028322	25.49	0.5098	50.98
6	460541.5	39.57222	0.039572	35.615	0.7123	71.23
8	539356.6	46.34444	0.046344	41.71	0.8342	83.42
10	615714.9	52.90556	0.052906	47.615	0.9523	95.23

Table 4: Stability report of the EGCG

Evaluation parameter	After 30 d	After 60 d	After 90 d
Colour and appearance	No change	No change	No change
% drug content	96.04±1.48	95.26±1.80	94.05±2.76
% drug release	94.08±2.25	93.87±1.27	93.14±1.38

Data are expressed mean±SD (n=3)

Table 5: Stability report of the berberine

Evaluation parameter	After 30 d	After 60 d	After 90 d
Colour and appearance	No change	No change	No change
% drug content	98.64±1.48	97.72±1.80	95.76±2.76
% drug release	95.23±1.97	94.98±2.64	93.71±1.45

Data are expressed mean±SD (n=3)

## CONCLUSION

In this research work, the EGCG+berberine combination was used as a model drug to be trapped in chitosan i.e. a natural biodegradable polymer using the gelation method. The results demonstrated that spherical-shaped nanoparticles were prepared successfully. The obtained nanoparticles exhibited narrow size distribution and high EE. The other characterization studies, such as DSC, and FT-IR confirmed the successful incorporation of EGCG+berberine into a polymeric matrix. The *in vitro* studies results demonstrated that the drug release profile follows the linearity to time. The *in vivo* studies are to be done to reach a concrete conclusion about the biological response, particularly anticancer effect.

## ACKNOWLEDGEMENT

The authors are thankful to Director Fr. Allam Arogya Reddy who provided the facility to carry out the work. The authors are also grateful to director National Institute of Technology, Tiruchirappalli for providing IR and DSC data. The authors express since thanks to Chromatogen analytical solutions for HPLC data.

## FUNDING

Nil

## AUTHORS CONTRIBUTIONS

All the authors have contributed equally.

## CONFLICT OF INTERESTS

Declared none

## REFERENCES

- Mohanraj V, Chen Y. Nanoparticles-a review. Trop J Pharm Res. 2006;5:561-73.
- Freitas Jr RA. Nanotechnology, nanomedicine and nanosurgery. Int J Surg. 2005;3(4):243-46. doi: 10.1016/j.ijssu.2005.10.007.
- Yih TC, Al-Fandi M. Engineered nanoparticles as precise drug delivery systems. J Cell Biochem. 2006;97(6):1184-90. doi: 10.1002/jcb.20796.
- Roque L, Castro R, Molpeceres R, Viana RS, Roberto A, Reis P. Bio adhesive polymeric nanoparticles as strategy to improve the treatment of yeast infections in oral cavity *in vitro* and *ex vivo* studies. Eur Polym J. 2018;104:19-31.
- Rizvi SAA, Saleh AM. Applications of nanoparticle systems in drug delivery technology. Saudi Pharm J. 2018;26(1):64-70. doi: 10.1016/j.jsps.2017.10.012, PMID 29379334.
- Vandervoort J, Ludwig A. Ocular drug delivery-nanomedicine applications. Nano Med. 2007;2:11-21.
- Jianghua L, Chao C, Jiarui L, Jun L, Jia L, Tiantian S. Chitosan-based nanomaterials for drug delivery. Molecules. 2018;23:1-26.
- Lehr CM, Bouwstra JA, Schacht EH, Junginger HE. *In vitro* evaluation of mucoadhesive properties of chitosan and some other natural polymers. Int J Pharm. 1992;78:43-8.
- He P, Davis SS, Illum L. *In vitro* evaluation of the mucoadhesive properties of chitosan microspheres. International Journal of Pharmaceutics. 1998;166(1):75-88. doi: 10.1016/S0378-5173(98)00027-1.
- Grenha A. Chitosan nanoparticles: a survey of preparation methods. J Drug Target. 2012;20(4):291-300. doi: 10.3109/1061186X.2011.654121, PMID 22296336.
- Wang J, Byrne JD, Napier ME, Desimone JM. More effective nanomedicines through particle design. Small. 2011;7(14):1919-31. doi: 10.1002/smll.201100442, PMID 21695781.
- Alonso MJ, Calvo P, Remunan Lopez C, Vila JLL. Novel hydrophilic chitosan polyethylene oxide nanoparticles as protein carriers. J Appl Polym Sci. 1998;63:125-32.
- Lu JJ, Bao JL, Chen JL, Huang M, Wang YT. Evidence-based complementary and alternative medicine. Nat Lib Med. 2012:1-12.
- Zhang C, Sheng J, Li G, Zhao L, Wang Y, Yang W. Effects of berberine and its derivatives on cancer: a systems pharmacology review. Front Pharmacol. 2019;10:1461. doi: 10.3389/fphar.2019.01461. PMID 32009943.
- Kumar GS. RNA targeting by small molecules-binding of protoberberine, benzo phenanthridine and aristolochia alkaloids to various RNA structures. J Bio Sci. 2012;37:539-52.
- Xiao N, Chen S, Ma Y, Qiu J, Tan JH, Ou TM. Interaction of berberine derivative with protein POT1 affect telomere function in cancer cells. Biochem Biophys Res Commun. 2012;419(3):567-72. doi: 10.1016/j.bbrc.2012.02.063, PMID 22369941.
- Moradzadeh M, Hosseini A, Erfanian S, Rezaei H. Epigallocatechin-3-gallate promotes apoptosis in human breast cancer T47D cells through down-regulation of PI3K/AKT and telomerase. Pharmacol Rep. 2017;69:924-28.

18. Nagle DG, Ferreira D, Zhou YD. Epigallocatechin-3-gallate (EGCG)-chemical and biomedical perspectives. *Phytochem*. 2006;67:1849-55.
19. Nakagawa K, Miyazawa T. Absorption and distribution of tea catechin, (-)-epigallocatechin-3-gallate, in the rat. *J Nutr Sci Vitaminol (Tokyo)*. 1997;43(6):679-84. doi: 10.3177/jnsv.43.679, PMID 9530620.
20. Nanjo F, Mori M, Goto K, Hara Y. Radical scavenging activity of tea catechins and their related compounds. *Biosci Biotechnol Biochem*. 1999;63(9):1621-23. doi: 10.1271/bbb.63.1621, PMID 10610125.
21. Akila RM, Maria Shaji D. Ginger loaded chitosan nanoparticles for the management of 3-nitropropionic acid-induced Huntington's disease-like symptoms in male wistar rats. *Int J Pharm Pharm Sci*. 2021;14(1):28-36. doi: 10.22159/ijpps.2022v14i1.42894.
22. El-Assal MI, Samuel D. Optimization of rivastigmine chitosan nanoparticles for neurodegenerative alzheimer-*in vitro* and *ex vivo* characterizations. *Int J Pharm Pharm Sci*. 2022;14(1):17-27.
23. Trinayan D, Das MK, Das S, Das P, Ronibala Singha L. Box-behken design approach to develop nano-vesicular herbal gel for the management of skin cancer in an experimental animal model. *Int J Appl Pharm*. 2022;14(6):148-66.
24. Joysa Ruby J, Pandey VP. Chitosan nanoparticles as a nasal drug delivery for memantine hydrochloride. *Int J Pharm Pharm Sci*. 2014;7(1):34-7.
25. E Elkholi I. Evaluation of anti-cancer potential of capsaicin-loaded trimethyl chitosan-based nanoparticles in HepG2 hepatocarcinoma cells. *J Nanomed Nanotechnol* 2014;5:6. doi: 10.4172/2157-7439.1000240.
26. Anbarasan B, Vennya V, Menon VA, Ramprabhu. Optimization of the formulation and *in vitro* evaluation of chloroquine-loaded chitosan nanoparticles using ionic gelation method. *J Chem Pharm Sci*. 2013;6:407-12.
27. Mali S, Oza N. Central composite design for formulation and optimization of long-acting injectable (LAI) microspheres of paliperidone palmitate. *Int J Appl Pharm*. 2021;13(5):87-98.
28. Manimekalai P, Manavalan R. Molecular docking studies of ceftriaxone sodium with apoptosis protein in colorectal cancer. *Int J Res Pharm SIC*. 2014;5:250-5.